PETROVIETNAM SCIENCE, TECHNOLOGY & INNOVATION PETROVIETNAM

INTEGRATION OF GEOLOGICAL AND WELL LOG AND GEOMECHANICAL MODELING TOWARD A SAFE MUD WEIGHT FOR WELLBORE STABILITY: A CASE STUDY OF RUBY FIELD, BLOCKS 01&02, CUU LONG BASIN

Nguyen Van Hoang[1], Nguyen Quoc Thap[2], Pham Quy Ngoc[3]
[1]Petrovietnam Exploration Production Corporation (PVEP)
[2]Vietnam Petroleum Association (VPA)
[3]Vietnam Petroleum Institute (VPI)
Email: ngocpq@vpi.pvn.vn
https://doi.org/10.47800/PVSI.2023.02-03

Summary

There is a high density of drilled wells in Blocks 01&02 which is a part of the Cuu Long basin. The geological settings of this area have undergone a complicated evolution, resulting in heterogeneous lithology and variable stresses. Consequently, drilling activities in the Ruby oil field have faced numerous challenges, such as stuck pipe, gas kick, mud loss, and even lost well, etc. leading to substantial time and financial setbacks. It is essential to thoroughly understand the geomechanical characteristics of Ruby field to ensure safe operation and optimize drilling. In this paper, several downhole geophysical data sets such as wireline logging data as gamma ray (GR), density log (RHOB), neutron (NPHI), compression/shear sonic travel time (DTC/DTS), image formation log (FMI), pressure test (MDT) and leak of test (LOT, XLOT) are used to construct the 1D geomechanical model. The objective of this modelling is to compute parameters of pore pressure, vertical stress, horizontal stress, elastics properties, rock strengths. Then, these parameters are used to analyze the wellbore stability and to recommend appropriate drilling mud weights for the wells under study. This analysis can subsequently be extended to cover the entire Ruby oil field for the future drilling operations to enhance overall safety and efficiency.

Key words: Geomechanical model, wellbore stability, mudweight, Cuu long basin

1. Introduction

The Ruby field, situated within the Cuu Long basin, has undergone a complex geological evolution, resulting in a zone characterized by lithological heterogeneity and varying stresses. Consequently, drillings in this area encountered various challenges such as stuck pipes, mud losses, and even lost wells, incurring significant financial and time expenses for the petroleum company. Therefore, it is crucial to comprehend the geomechanical properties of the rocks in this study area to prevent well damages and optimize the drilling costs. This study aims to construct a 1D geomechanical model to calculate vertical stress, pore pressure, horizontal stress, elastic properties and rock strengths. Wireline logging data in Ruby field including gamma-ray (GR), density log (RHOB), neutron log (NPHI), shear slowness travel time (DTS), compressive slowness travel time (DTC), image logs, pore pressure tests (MDT/RFT) and data of leak of test, extended leak of test or mini-frac for the identification of minimum horizontal stress, are utilized in this modeling process. Finally, the results from the 1D geomechanical model are employed to analyze wellbore stability and recommend drilling mud weights for the upcoming wells in the Ruby field.

Date of receipt: 23/10/2023. Date of review and editing: 23/10 - 24/11/2023.
Date of approval: 7/12/2023.

2. Background

Up to now, 85% of oil and gas production in Vietnam primarily comes from fields in the Cuu Long basin [1], marking the crucial role of this basin in the country's oil and gas industry. The Cuu Long basin is a typical rift basin that has been undergoing a complexity of tectonic evolution including pre-rifting, rifting and thermal subduction mechanisms [2]. These tectonic activities contributed to the formation of various types of rocks with different lithological components corresponding to different rock

facies, depositional environments and buried conditions, leading to differences of geomechanical properties such as pore pressure, stresses, etc. Therefore, many challenges need to be addressed during drilling, such as bore hole wall collapse, total circulation losses, stuck pipe/logging tools, etc. Because of these problems, the petroleum company may suffer critical loss financially due to an increase in non-productive time, e.g. solving and fixing problems, leading to higher drilling costs. In order to fix these problems, it is a must to minimize non-productive time related to wellbore instability and undesired issues caused by the pore pressure mechanism of formations. This is a complex task that needs to be proposed before drilling and updated during and after drilling. This task includes the assessment of drilling risks, identifying geological variations at the wellbore to develop contingency plans for unforeseen issues [3]. Therefore, understanding the geomechanical properties of rocks plays an increasingly important role in solving the problem of wellbore instability, optimizing well costs, and ensuring safety in drilling progress.

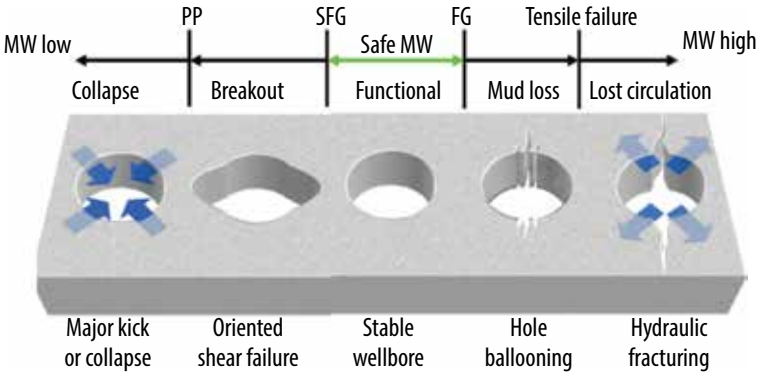

Figure 1. *The influence of pressure and drilling mud weight on the wellbore conditions [4].*

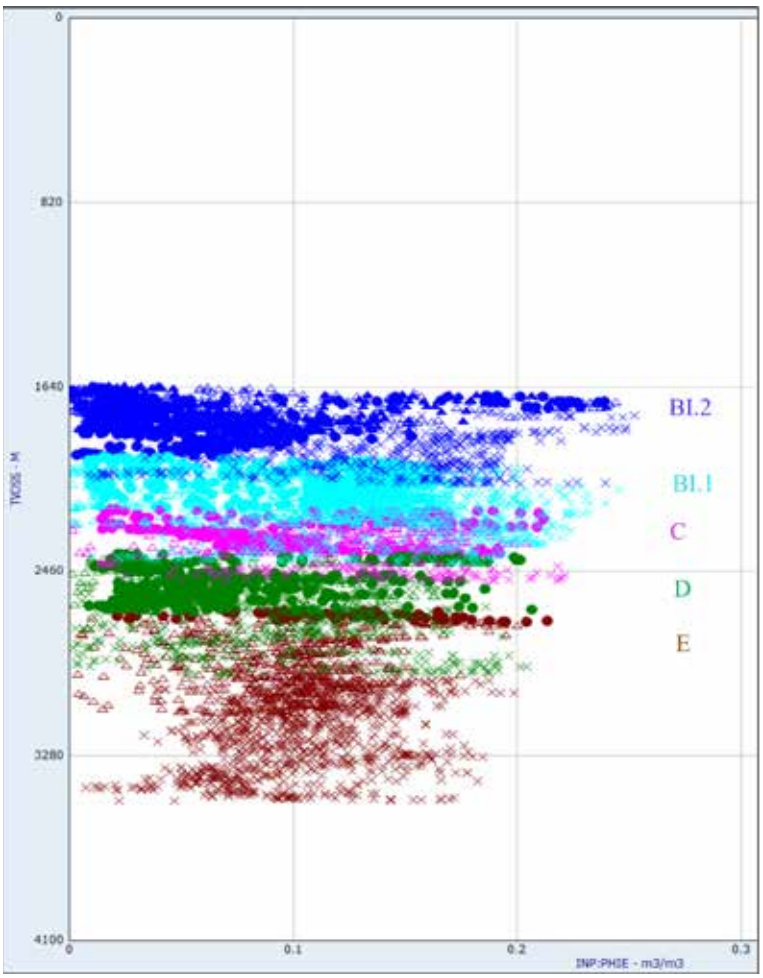

Figure 2. *The porosity versus the depth in some well in Ruby field, Blocks 01&02, Cuu Long basin.*

Throughout drilling progress, the cuttings are removed by drilling bit; the drilling fluid will be brought to the surface, and immediately replace equally the volume of the excavated formation; the stresses around the wellbore will be redistributed, and induced stresses will also be generated. To ensure the wellbore stability, the drilling mud weight must be consistent with controlling the induced wellbore stresses. In more details, the shear stress and tensile are the main factors that cause the mechanical instability of the wellbore [4]. Obviously, if the drilling mud weight is high, it will create induced fractures causing mud loss, called tensile failure; but on the contrary, if it is too low, it will lead to wellbore collapse, called shear failure (Figure 1).

The selection of the mud weight should be greater than the pore pressure but less than fracture pressure. This is a principle in wellbore designation and identification of casing depths, saving several millions of dollars when applied to design casing shoes [5]. In this paper, the authors will use wireline logging data including gamma ray, density log, resistivity log, sonic log, in conjunction with drill stem tests (DSTs), LOT, MDT, drilling events, and production data from the Ruby field, Blocks 01&02, Cuu Long basin. This comprehensive dataset will be used to construct the 1D geomechanical model (1D MEM), providing parameters such as the pore pressure, formation stresses and mud weight windows [6]. Afterward, this model continues to be updated and refined with the future wells to ensure the minimization of drilling

incidents and optimization of the drilling operations and associated production progress.

3. Geological settings of the Ruby field.

The research area is the oil field named Ruby in Blocks 01&02, located in the Northeast of Cuu Long basin. There are 37 drilled wells in the field, comprising 4 exploration wells and 33 production wells. The hydrocarbon-bearing formations consist of consolidated sand reservoirs with effective porosity ranging from 18 - 23% in the Miocene and 11 - 20% in the Oligocene (Figure 2).

Oil flows from DST results and production in the Oligocene to Miocene formations mostly show characteristics of oil in the study area, which is the relatively light oil with API from 39 to 44 degree.

Rifting, compression, and thermal subduction are primarily typical tectonic activities in the Cuu Long basin and particularly in the research area (Figure 3).

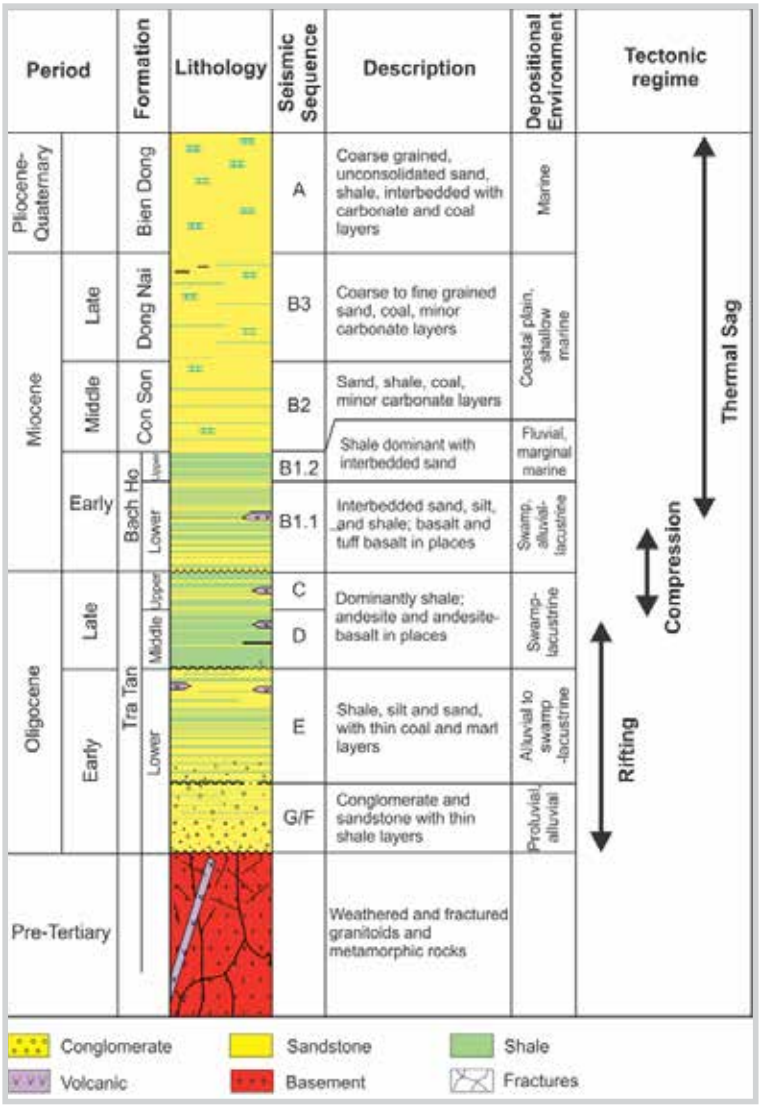

Figure 3. *Lithological and stratigraphic column of the Ruby field [7, 8].*

Onset of the rifting progress commenced from Eocene to early Oligocene [9], giving rise to a series of narrow, localized basins oriented in the NE - SW and E - W directions. Subsequently, the study region experienced alternating phases of compression and rifting during the transition from the late Oligocene to the early Miocene, with a predominant NE - SW orientation. Particularly, the basin was continuously compressed, leading to the creation of a series of reverse faults, notably encountered in Bach Ho, Diamond field [10]. The tectonic progresses mentioned above had created a sedimentary basin with closed boundaries, resembling a large lake [2, 7]. Finally, the Cuu Long basin has been undergoing thermal subduction from the early Miocene to the present, representing a relatively stable phase and a significant influence of the marine environment.

The strata of Blocks 01&02 are relatively similar to those in the Cuu Long basin, as mentioned by previous studies. According to Tran Le Dong and Tran Dac Hoai [8], a stratigraphic and lithological column refers to a graphical representation or chart that depicts the geological formations in a specific area. In this context, the column includes both the pre-Tertiary fractured basement and Tertiary sedimentary rocks. The construction of this column involves detailing the characteristics of petrography, fossils, and sedimentation for each stratigraphic unit. Figure 3 is likely a visual representation accompanying this construction, providing a detailed illustration of the geological layers and their respective features in the studied region. Six sedimentary sequences, labeled from F to A, are identified, along with one pre-Tertiary fractured basement unit. Below is a brief description of both the basement and the overlying clastics:

- The Tertiary basement rocks consist of intrusive crystallized granite rocks, contemporaneous with three complexes: Hon Khoai, Dinh Quan, and Ca Na [8].

- The F sequence (or G sequence with local distribution) spans from the Eocene to the lower Oligocene, constituting the earliest

formation and likely present in the deepest sections of the Cuu Long basin. This formation comprises lithological elements such as sandstones, conglomerates, siltstones, and interspersed thin shales. These deposits originated in a high-energy environment, characterized as alluvial and proluvial.

- The E sequence, dating to the early upper Oligocene, is composed of well-sorted to fine-grained sandstones along with thin conglomerates, siltstones, and interbedded shale.

- The D sequence, dating to the middle upper Oligocene, predominantly comprises sandstones, silt, and shale. These sediments were deposited in swampy, alluvial, and lacustrine environments..

- The C sequence, dating to the late upper Oligocene, is primarily composed of sandstones with varying grain sizes, including medium, fine, and very fine grains. These sandstones are interbedded with silt and claystones, and they were deposited in deltaic plains and lacustrine environments. Additionally, they completely filled the remaining lakes within the rift basin.

- The sedimentary sequences, dating from the late Oligocene to the Miocene B, are primarily composed of shale with interbedded sandstones and minor carbonate layers. These sediments were deposited in swampy, lacustrine, and shallow marine environments.

- The sedimentary sequence A, spanning from the Pliocene to Quaternary A, is characterized by coarse-grained, unconsolidated sandstones interbedded with shale, carbonate, and coal layers [7].

4. Fundamental theory for constructing a 1D geomechanical model from geological and wireline logging

The 1D geomechanical model (1D MEM) comprises mechanical, elastic properties of rocks and states of in-situ stresses along the wellbore [11]. Fundamentally, the 1D geomechanical model uses geological and various wireline logging data to obtain vertical stress (σ_v), pore pressure P_p, elastic properties including shear (G_{dyn}) and bulk K_{dyn} modulus, Young's modulus E and Poisson's ratio (ϑ). It also calculates rock strengths such as uniaxial compressive stress UCS, tensile TS, friction angle FANG, minimum σ_{hmin} and maximum σ_{Hmax} horizontal stresses.

There is a workflow to construct 1D MEM model as following:

(i) Review and collection of data. In this research, the

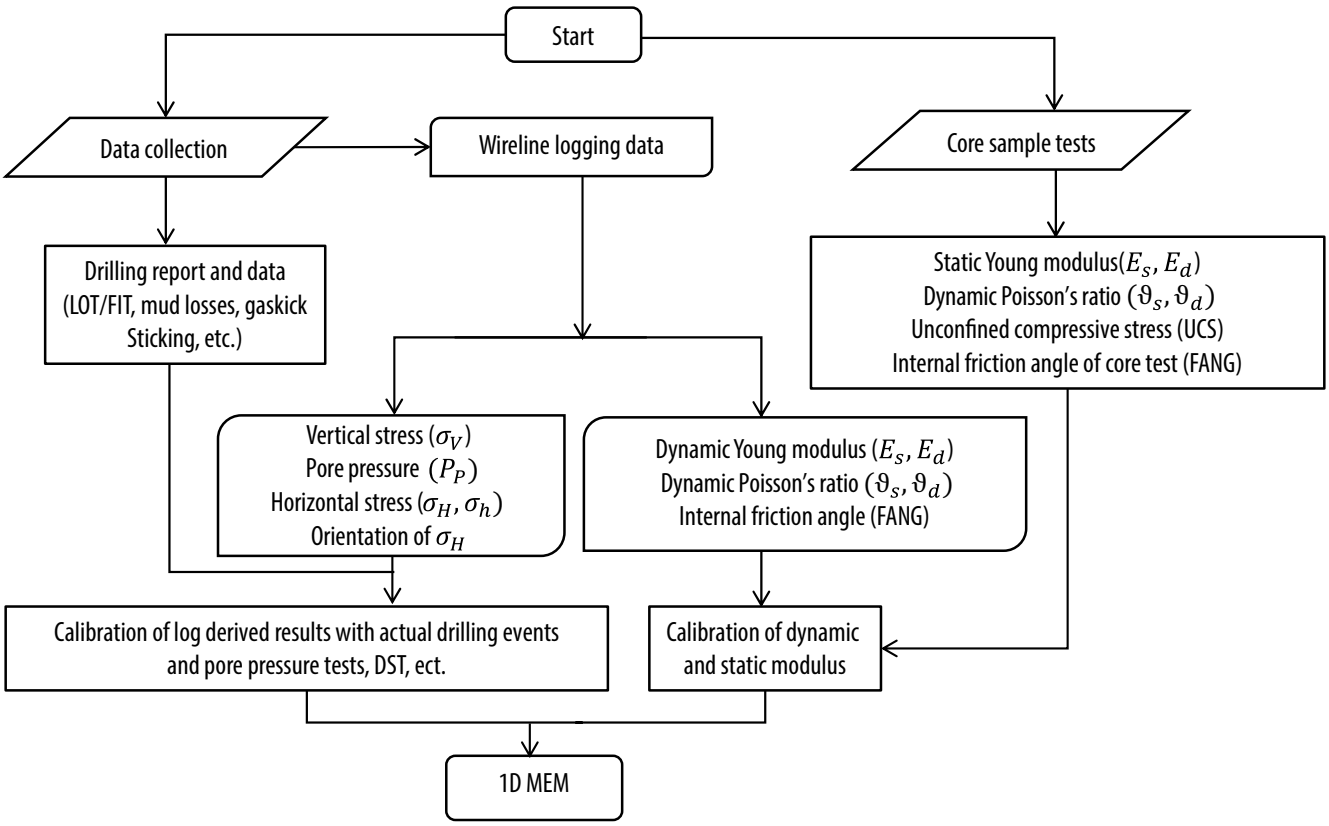

Figure 4. *Workflow for determination of the 1D MEM geomechanical model.*

authors review and collect wireline logging data in Blocks 01&02, the Northern East part of Cuu Long basin. The data encompass completion well data, drilling reports, laboratory core tests and wireline logging data such as gamma ray (GR), caliper log, density log (RHOB), neutron (NPHI), compression/shear sonic travel time (DTC/DTS), image formation log (FMI), pressure test (MDT) and leak of test (LOT, XLOT).

(ii) Determination of vertical stress, pore pressure, magnitude and orientation of maximum horizontal stress, magnitude of minimum horizontal stress.

(iii) Determination of elastic parameters, rock strengths, and final interpretation of the failure of the rocks (Figure 4).

4.1. Determination of vertical stress and pore pressure

- Vertical stress

The vertical stress (psi) or overburden stress (σ_V) is the pressure exerted on a formation at a given depth due to the total weight of the rocks and fluids above that depth and derived by Equation (1) [12]:

$$\sigma_V = \rho_w . z_w . g + \int_0^z \rho_b(z) . g . dz \quad (1)$$

where ρ_b, ρ_w are density of rocks (RHOB) and density of fluid in g/cm^3; g is the gravity acceleration in m/s^2; z and z_w are respectively vertical depth and sea water height in meters. Normally, density log is not measured fully along a wellbore. Therefore, the density data must be filled for gap intervals using several empirical correlations. One of those frequently used to process is the extrapolation density method. Mostly, the density of seawater and average density of rocks are 1.03 g/cm^3 and 2.3 g/cm^3, respectively [12].

- Pore pressure

Pore pressure is the pressure of fluids in the pore space of rocks. It is one of the most important parameters of exploration and production wells. According to Eaton's method, the pore pressure (psi) is determined from the vertical stress and sonic log as follows [13, 14]:

$$P_p = \sigma_V - (\sigma_V - P_{p\_norm}) . (\frac{DT_{obser}}{DT_{norm}})^3 \quad (2)$$

Where P_p is the pore pressure; P_{p_norm} is hydrostatic pressure in psi; DT_{obser} is the measured log (DTC); DT_{norm} is the normal compaction trend, in ms/ft. Afterward, the results of pore pressure will correlate with pore pressure points which are measured directly from MDT/DFT/RCI logs or DST results.

4.2. Elastic properties of the rocks

- Elastic parameters

The elastic parameters are necessary to construct the 1D geomechanical model and encompasses Young's modulus, Poisson ratio, shear modulus and bulk modulus [11]. In fact, the values of Young's modulus and Poisson's ratio calculated from the wireline logs are normally greater than those obtained from laboratory core tests. Therefore, it is needed to calculate Young's modulus and Poisson dynamic modulus [15], as follows:

$$E_{Dyn} = \frac{9G_{dyn} \times K_{dyn}}{G_{dyn}+3K_{dyn}} \quad (3)$$

Dynamic Young's modulus (E_{Dyn}) is a parameter indicating the deformation characteristics of rocks along any axis. It represents a capacity of rocks resisting elastic deformation.

$$\vartheta_{Dyn} = \frac{3K_{dyn}-2G_{dyn}}{2G_{dyn}+6K_{dyn}} \quad (4)$$

Where:

Dynamic shear modulus (G_{dyn}), shown below, is also known as the modulus of rigidity, a measure of the sample's resistance to shear deformation.

$$G_{dyn} = \frac{\rho_b}{DTC^2} \quad (5)$$

- Dynamic bulk modulus (K_{dyn}), shown below, is a measurement of the sample's resistance to hydrostatic compression.

$$K_{dyn} = \frac{\rho_b}{DTC^2} - \frac{4}{3}G_{dyn} \quad (6)$$

Derived parameters from wireline logs are terms of the dynamic elastic moduli. These values must be converted to the static elastic moduli through a correlation which is shown in Equations (7), (8) below [16].

$$E_{sta} = 0.032 \times E_{dyn}^{1.632} \quad (7)$$

$$\vartheta_{sta} = \vartheta_{Dyn} \quad (8)$$

- Rock strengths

Uniaxial compressive stress (UCS): The compressive strength is probably the most widely used and quoted rock engineering parameter. It is the maximum axial compressive stress that rocks can withstand before failure, denoted as UCS, in psi. The UCS values of rocks are determined through uniaxial compressive tests. In addition, there are many methods to calculate the unconfined compressive stress [17]. J.Fuller [16, 18] proposed a correlation between UCS and the slowness of travel time of rocks.

$$UCS = 0.77 \times (\frac{304.8}{DTC})^{2.93} \quad (9)$$

+ Tensile failure (*TS*), in psi: It is the maximum strain stress that rocks can withstand before failure, denoted as *TS*. Tensile strength normally assumes to be 1/10 values of *UCS* [19, 20].

+ Internal friction angle (*FANG*), in degree: It is a characteristic parameter representing shear resistance of the rocks, describing the shear resistance due to a friction of rocks with effective stress at an angle. Friction angle is a function of porosity and clay volume which was proposed by Plumb [11].

$$FANG = 26.5 - 37.4(1 - \Phi - V_{cl}) + 62.1(1 - \Phi - V_{cl})^2 \quad (10)$$

+ Minimum horizontal stress and maximum horizontal stress, in psi: These are magnitudes of minimum and maximum compressive stresses in the horizontal direction, denoted as σ_{hmin} and σ_{Hmax}, respectively. In the field, values of σ_{hmin} can be referred to using LOT, XLOT and minifrac data from drilling wells [21]. Additionally, σ_{hmin}, σ_{Hmax} can be estimated from wireline logs (11), (12) [11, 16]

$$\sigma_{hmin} = \frac{\vartheta}{1-\vartheta}\sigma_V + \frac{1-2\vartheta}{1-\vartheta}\alpha P_p + \frac{E}{1-\vartheta^2}\varepsilon_h + \frac{\vartheta E}{1-\vartheta^2}\varepsilon_H \quad (11)$$

$$\sigma_{Hmax} = \frac{\vartheta}{1-\vartheta}\sigma_V + \frac{1-2\vartheta}{1-\vartheta}\alpha P_p + \frac{E}{1-\vartheta^2}\varepsilon_H + \frac{\vartheta E}{1-\vartheta^2}\varepsilon_{min} \quad (12)$$

+ Azimuth angle of the maximum horizontal stress: This parameter is determined by using wellbore image logs such as FMI, FMS, CBIL, ect. These are useful methods for determining the orientation of the maximum horizontal stress σ_{Hmax}. Analyzing wellbore image logs can show occurrence of faults, fractures yielding three types of structures: (1) Sinusoidal shape clearly visible around wellbore which marks plane fault or foliation planes. (2) Pairs of traces parallel to the wellbore axis offset by 180° and not interconnected around the wellbore wall are called drilling induced tensile wall fractures because they are formed during the drilling process as pure tensile fractures but do not appear to propagate significantly into the rock surrounding the borehole, and therefore are limited to the borehole wall. (3) Fracture traces 180° offset at their borehole wall but inclined with respect to the borehole axis [22]. The well used for this study lack of the wellbore image data. Therefore, the determination of the orientation of the maximum horizontal stress is based on references from surrounding area (Figure 5). Figure 5 indicates that the orientation of the maximum horizontal stress is N138+/-12.

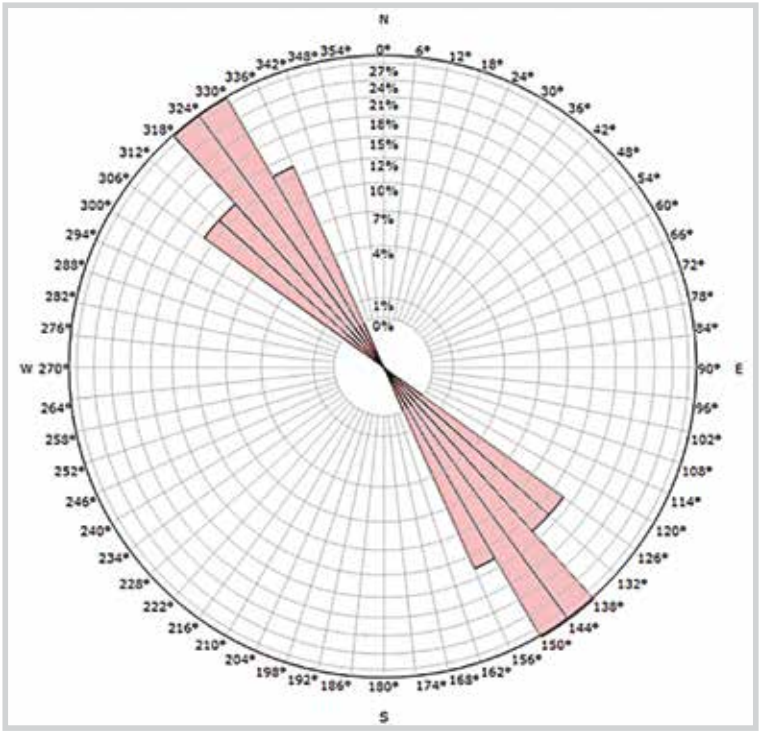

Figure 5. *The orientation of the maximum horizontal stress is referred surrounding area indicating an azimuth of N138 +/-12°.*

5. A case study of 1D geomechanical model for well Y-1 in Ruby field

The 1D geomechanical model is constructed for a well in the study area. Its results are quite similar to actual events that occurred during drilling processes such as breakout intervals, stuck or tight holes, etc. Figure 6 illustrates drilling progressive and drilling problems in well Y-1. It is noted that in the depth interval from 1,600 - 2,300 m with hole diameter of 12.25 inches, the drilling mud weight was applied as high as 10.0 ppg. However, a series of problems was taken place, such as tight spots and mud losses, prompting the petroleum operator to adjust the mud weight to 9.5 ppg. Nevertheless, well Y-1 continues to experience mud dynamic losses, and connection gases. In the section 8.5 inches, the mud weight increases from 9 ppg to 10.5 ppg. However, the well still encounters tight spots and stuck pipes, and then the wellbore gets more stability when mud weight increases further to 10.6 ppg despite some minor losses. Then, there are some tight spots when running the 7 inch liners.

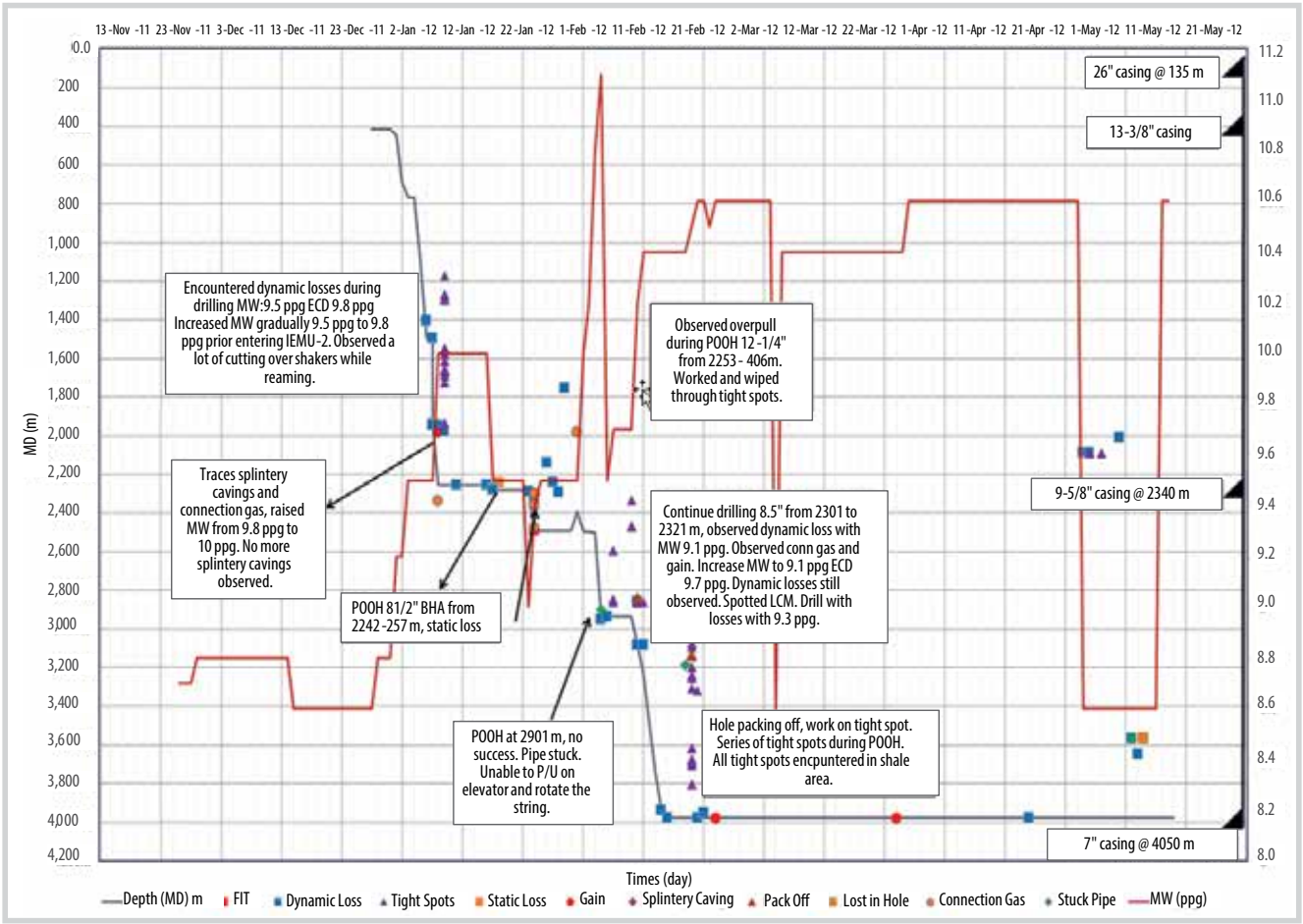

Figure 6. *Time verse depth chart of well Y-1, as shown incidents during drilling.*

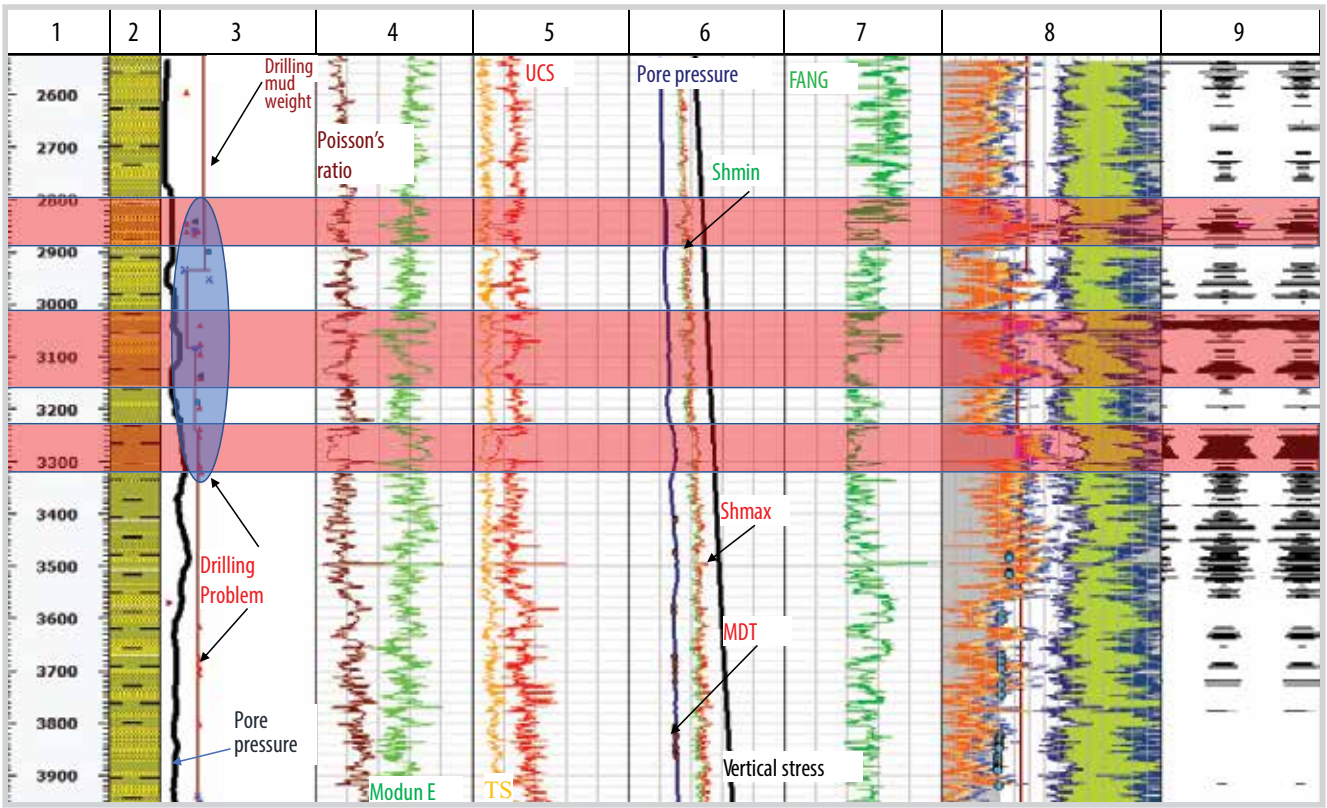

Figure 7. *Displaying outputs of the 1D geological model for well Y-1.*

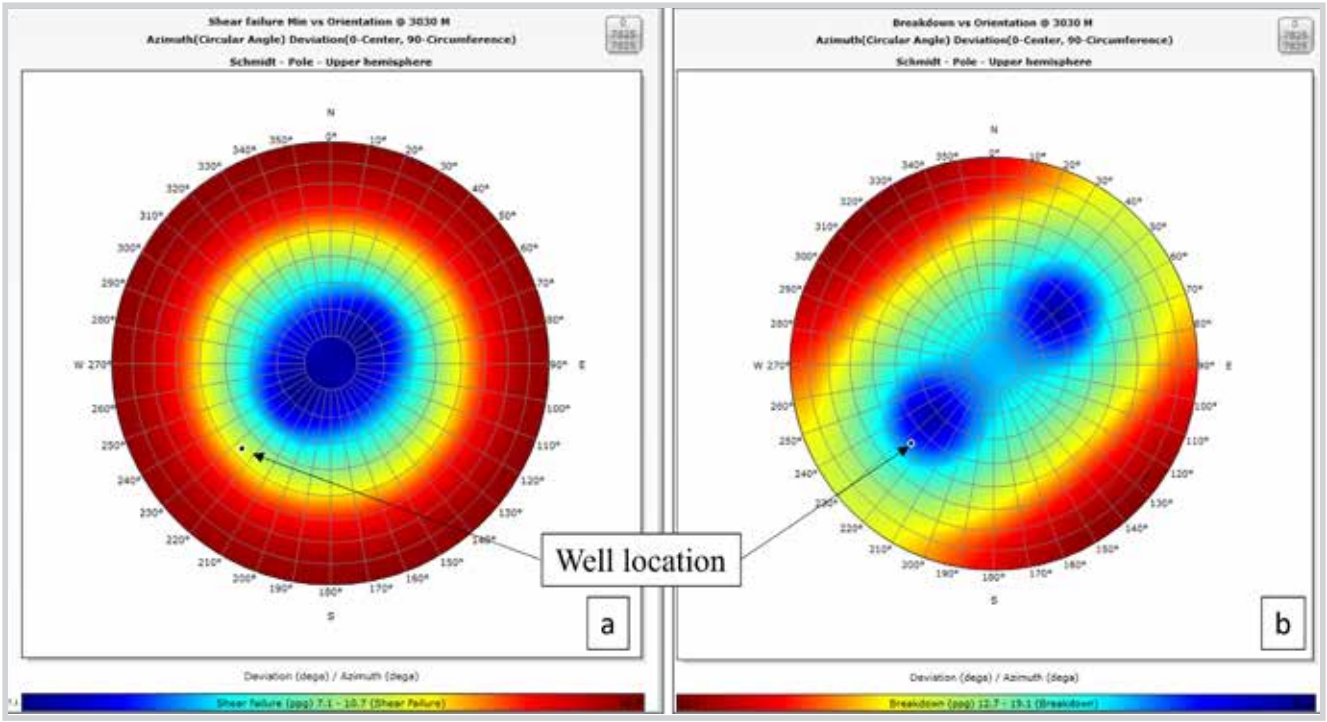

Figure 8. *The sensitivity of mud weight at a depth of 3,330 mMD: (a) No experience fracture failure; (b) Strongs washouts.*

Table 1. *Parameters of the 1D geomechanical model in depths of well Y-1*

Well status vs applied mudweight				Results of 1DMEM and Proposed Mudweight									
Depth (mMD)	Lithology	Used mudweight (ppg)	Well status	Pore pressure Gradient (psi/ft)	Vertical Gradient (psi/ft)	Shmin (psi)	Shmax (psi)	Poisson (frac)	Young E (pdi)	UCS (psi)	TR (psi)	FANG (deg)	Proposed mudweight (ppg)
2,750	Shale	10.80	Good	3240.58	3886.26	5019.00	5293.00	0.29	0.89	5391.2	539.20	30.60	10.80
2,800	Sand	10.80	Good	3297.60	7002.00	4927.60	5263.00	0.27	1.06	5744.8	574.40	34.90	10.80
2,850	Shale	10.80	Breakout	3558.50	7120.00	4632.90	4736.20	0.32	0.22	1779.2	177.90	19.00	11.40
3,120	Shale	10.20	Breakout	3851.60	7761.10	6205.20	6319.40	0.39	0.36	3558.2	335.80	19.20	12.00
3,280	Shale	10.40	Breakout	4415.30	8146.40	6581.40	6700.00	0.40	0.35	3352.7	335.20	23.30	12.00
3,500	Sand	10.40	Breakout	4583.40	8676.90	7395.20	7487.20	0.30	0.39	3849.2	384.90	19.00	11.70
3,630	Sand	10.40	Breakout	4381.10	9024.00	6866.00	7046.50	0.60	0.33	4327.7	432.70	20.80	11.00
3,900	Sand	10.40	Good	4668.70	9810.80	6816.50	7267.00	1.40	0.25	7064.2	706.40	27.90	10.40

Figure 7 shows the outputs from 1D geomechanical model. Track #6 shows parameters of vertical stress, pore pressure, maximum and minimum horizontal stresses; Poisson's ratio and Young's modulus are expressed in track #4, while track #5 shows parameters of uniaxial compressive stress and tensile strength. Track #7 exclusively shows parameters of internal friction angle. Tracks #8 and 9 display the mud weight windows and breakout intervals. Track #3 records the mud weight used during drilling.

The interval of the study in the well ranges from 2,500 m to approximately 4,000 m with lithological components comprising sandstones interbedded and dominantly claystones.

There are some problems encountered while drilling, which are marked in red zones in depth intervals of 2,800 - 2,900 m, 3,020 - 3,187 m and 3,230 - 3,310 m. In these intervals, the drill mud weight is set down, from 10.4 ppg to 9.7 ppg, and then back to 10.4 ppg. Despite the similar mud weight applied, a series of drilling problems are still encountered, including tight spots, collapse, sticking and even gaskicks. Comparing the pore pressure calculation results to the applied drilling mud weight, there is a difference greater than 1 - 1.5 ppg, yet the wellbore wall remains unstable. Comparing the results of the 1D geomechanical model to the applied mud weight indicates that the wellbore wall is still experiencing breakout, collapsing that agrees with actual drilling events. Nevertheless, the 1D geomechanical model also suggests

proper mud weights for each interval: 10 ppg for 2,500 - 2,810 m, 12 - 12.5 ppg for 2,810 - 3,550 m, respectively. The remaining intervals of the wellbore should have a reduced mud weight to around 11.7 - 11.5 ppg.

The sensitivity analysis of the mud weight regarding potential of breakout and fracture failure due to the inclination and the azimuth of the wellbore is carried out at a depth of 3,330 m. The result indicates that the wellbore is able to wash out strongly but not cause fracture failure, as illustrated in Figure 8.

The calculation results of the 1D geomechanical model are shown in depths of well Y-1 in Table 1.

6. Conclusions

The research area is located in the Northeast of Cuu Long basin, which is formed through complex tectonic evolutions from the pre-Tertiary to the present. It is a typical rift basin where rifting activities have been undergoing from the Eocene to the late Oligocene. There is also a short time period of compression from the late Oligocene to the early Miocene, though not very intense. Being considered to mainly undergo thermal subduction, the Cuu Long basin is therefore characterized by a normal fault regime with stress field $\sigma_V > \sigma_{Hmax} > \sigma_{hmin}$. The results of well Y-1 have a series of drilling problems relating to drilling mud weights such as sticking pipe, tight spots, gas kick, mud losses, breakout, etc. This study is based on geological and wireline logging data to calculate and construct the 1D geological model to determine parameters of vertical stress, pore pressure, elastic properties (Young's modulus, Poisson's ratio), minimum and maximum horizontal stresses, unconfined compressive stress and mud window for each interval of well Y-1. The mud weight for each interval should be set around 10 - 12.5 ppg.

Acknowledgement

The authors are grateful to the Ministry of Industry and Trade (under Contract No. 006.2021.CNKK.QG/HDKHCN on 3 February 2021) and Vietnam Petroleum Institute (VPI) for their support and provision of financial resources for this study.

References

[1] Nguyen Van Dac, "Chapter 3: Overview of petroleum resources of Vietnam", In: *The Petroleum Geology and Resources of Vietnam*. Science and Technics Publishing House, 2005.

[2] Le Van Cu, Hoang Ngoc Dang, and Tran Van Tri, "Chapter 5: Tertiary sedimentary basins in Vietnam". In: *The Petroleum Geology and Resources of Vietnam*. Science and Technics Publishing House, 2005.

[3] Richard Plumb, Stephen Edwards, Gary Pidcock, Donald Lee, Brian StaceyThe mechanical earth model concept and its application to high-risk well construction projects", *IADC/SPE Drilling Conference, New Orleans, Louisiana, 23 - 25 February 2000*. DOI: 10.2118/59128-MS.

[4] Ayoub Darvishpour, Masoud Cheraghi Seifabad, David Anthony Wood, and Hamzeh Ghorbani, "Wellbore stability analysis to determine the safe mud weight window for sandstone layers", *Petroleum Exploration and Development*, Vol. 46, No. 5, pp. 1031 - 1038, 2019. DOI: 10.1016/S1876-3804(19)60260-0.

[5] Daniel Moos, Pavel Peska, Thomas Finkbeiner, and Mark Zoback, "Comprehensive wellbore stability analysis utilizing", *Journal of Petroleum Science and Engineering*, Volume 38, Issues 3 - 4, pp. 97 - 109, 2003. DOI: 10.1016/S0920-4105(03)00024-X.

[6] M.S. Asadi, A. Khaksar, M.J. Ring, and K. Yin Yin, "Comprehensive geomechanical modeling and wellbore stability analysis for infill drilling of high-angled wells in a mature oil field", *SPE Asia Pacific Oil & Gas Conference and Exhibition, Perth, Australia, 25 - 27 October 2016*. DOI: 10.2118/182220-MS.

[7] William J. Schmidt, Bui Huy Hoang, James W. Handschy, Vu Trong Hai, Trinh Xuan Cuong, and Nguyen Thanh Tung, "Tectonic evolution and regional setting of the Cuu Long basin, Vietnam", *Tectonophysics*, Volume 757, pp. 36 - 57, 2019. DOI: 10.1016/j.tecto.2019.03.001.

[8] Tran Le Dong and Phung Dac Hai, "Chapter 9: Cuu Long sedimentary basin and petroleum resources", In: *The Petroleum Geology and Resources of Vietnam*. Science and Technics Publishing House, 2005.

[9] Michael B.W. Fyhn, Lars O. Boldreel, and Lars H. Nielsen, "Geological development of the Central and South Vietnamese margin: Implications for the establishment of the East Sea, Indochinese escape tectonics and Cenozoic volcanism", *Tectonophysics*, Volume 478, Issues 3 - 4, pp. 184 -214, 2009. DOI: 10.1016/j.tecto.2009.08.002.

[10] Trinh Xuan Cuong and J. K. Warren, "Bach Ho field, a fractured granitic basement reservoir, Cuu Long basin, offshore SE Vietnam: A "buried-hill" play", *Journal of Petroleum Geology*, Volume 32, Issue 2, pp. 129 - 156, 2009. DOI: 10.1111/j.1747-5457.2009.00440.x.

[11] Muhammad Zain-Ul-Abedin and Andreas Henk, "Building 1D and 3D mechanical earth models for underground gas storage - A case study from the Molasse basin, Southern Germany", *Energies*, Volume 13, Issue 21, 2000. DOI: 10.3390/en13215722.

[12] M. Zoback, "Part I: Basic principles", In: *Reservoir Geomechanics*. Cambridge University Press, 2007. DOI: 10.1017/CBO9780511586477.

[13] Milendra Prankada, Kriti Yadav, and Anirbid Sircar, "Analysis of wellbore stability by pore pressure prediction using seismic velocity", *Energy Geoscience*, Volume 2, Issue 4, pp. 219 - 228, 2021. DOI: 10.1016/j.engeos.2021.06.005.

[14] Nguyen Van Hoang, Pham Quy Ngoc, Nguyen Minh Quy, and Doan Huy Hien, "Pre-drill pore pressure prediction using seismic interval velocity and wireline log: Case studies for some wells in Cuu Long and Song Hong basins", *Petrovietnam Journal*, Volume 8, pp. 5 - 12, 2022. DOI: 10.47800/PVJ.2022.08-01.

[15] Mohammed S. Ameen, Brian G.D. Smart, J.Mc. Somerville, Sally Hammilton, and Nassir A. Naji, "Predicting rock mechanical properties of carbonates from wireline logs (A case study: Arab-D reservoir, Ghawar field, Saudi Arabia", *Marine and Petroleum Geology*, Volume 26, Issue 4, pp. 430 - 444, 2009. DOI: 10.1016/j.marpetgeo.2009.01.017.

[16] Schlumberger, "*Schlumberger techlog software solution*", 2021.

[17] Chandong Chang, Mark D. Zoback, and Abbas Khaksarb, "Empirical relations between rock strength and physical properties in sedimentary rocks", *Journal of Petroleum Science and Engineering*, Volume 51, Issues 3 - 4, pp. 223 - 237, 2006. DOI: 10.1016/j.petrol.2006.01.003.

[18] Per Horsrud, "Estimating mechanical properties of shale from empirical correlations. *SPE Drilling & Completion*, Volume 16, Issue 2, pp. 68 - 73, 2001. DOI: 10.2118/56017-PA

[19] Saeed Shad, Parvin Kolahkaj, and Davood Zivar, "Geomechanical analysis of an oil field: Numerical study of wellbore stability and reservoir subsidence", *Petroleum Research*, Volume 8, Issue 3, pp. 350 - 359, 2023. DOI: 10.1016/j.ptlrs.2022.08.002.

[20] Ramli Nazir, Ehsan Momeni, Danial Jahed Armaghani, and Mohd For Mohd Amin, "Correlation between unconfined compressive strength and indirect tensile strength of limestone rock samples electronic", *Journal of Geotechnical Engineering*, Volume 18, pp. 1737-1746, 2013.

[21] Mark D. Zoback, "Part II: Measuring stress orientation and magnitude", In: *Reservoir Geomechanics. Cambrigde University Press*, 2007. DOI: 10.1017/CBO9780511586477.

[22] M. Brudya M.D. Zoback, "Drilling-induced tensile wall-fractures: implications for determination of in-situ stress orientation and magnitude", *International Journal of Rock Mechanics and Mining Sciences*, Volume 36, Issue 2, pp. 191 - 215, 1999. DOI: 10.1016/S0148-9062(98)00182-X.